AFM Study of Lamellar Structure of Melt-Crystallized *n*-Alkane $C_{390}H_{782}$

A. Tracz*,† and G. Ungar*,‡

Centre of Molecular and Macromolecular studies, Polish Academy of Science, Sienkiewicza 112, 90 -363 Lodz, Poland, and Department of Engineering Materials, University of Sheffield, Sheffield S1 3JD, UK

Received March 8, 2005
Revised Manuscript Received April 29, 2005

Introduction. Long chain monodisperse normal alkanes with between 100 and 390 carbons are important models in studies of polymer crystallization.[1] Their structure and morphology have been studied by scattering methods,[2−4] spectroscopy,[5−7] and microscopy (TEM,[8,9] AFM,[10−12] optical[13]). Unlike polyethylene (PE), the thickness of the crystalline lamellae assumes quantized values corresponding to the integer fractions (1, 1/2, 1/3, ..., 1/n) of the projection of the molecular contour length (L) onto the lamellar normal.[14] Such "integer folded forms" are referred to hereafter as E (for $n = 1$), F2 ($n = 2$), F3 ($n = 3$), etc. Crystallization from the melt at temperatures below the melting point of F2 was found to proceed via a transient "noninteger form" (NIF).[15]

Previous studies of long alkane single crystals by AFM have focused on the morphological changes on annealing of solution-grown crystals. They revealed preferential lamellar thickening at crystal edges and the formation and migration of holes[10,11] as well as epitaxial recrystallization of lamellae at right angle to the initial lamella and the fold planes.[12] Furthermore, it was shown on the example of alkane $C_{390}H_{782}$ that a monomolecular layer of extended chains lying flat on the graphite surface in parallel ribbons has a "melting" point of 185 °C, compared to 132 °C for extended chain bulk crystals. Previous work on shorter alkanes has also shown increased stability of the ordered monolayer on graphite surface.[16,17]

The objective of the present study is to find whether and to what extent the structure of this monolayer is carried through into the bulk during crystallization. More generally, we aim to establish and apply a technique capable of probing the interior of bulk crystallized material by a high-resolution real-space method such as AFM. For this purpose we have investigated the morphology of alkane $C_{390}H_{782}$ using the substrate detachment technique developed for studies of melt-crystallized PE.[18−20] The surface of the polymer sample crystallized in contact with an atomically flat substrate is exposed by gentle detachment from the substrate and then investigated by AFM.

Experimental Section. *n*-Alkane $C_{390}H_{782}$ was synthesized by Dr. G. M. Brooke and co-workers at the University of Durham.[21] It was molten at 150 °C in contact with freshly cleaved highly oriented pyrolytic graphite (HOPG, SPI Supplies). After 10 min the sample was cooled at 10 °C/min. The graphite substrate was then cleaved off the sample, a notch having been initiated with a razor blade. Subsequently, the exposed surface was investigated using a Nanoscope IIIa atomic force microscope (Digital Instruments/Veeco) operated in tapping mode. Rectangular silicon cantilevers model RTESP7 (Nanosensors, Wetzlar-Blankenfeld, Germany) were used throughout the study. The AFM was calibrated laterally using the standard calibration grid purchased from Veeco. Height calibration was performed using HOPG surface with thermally etched monolayer pits (step height 0.335 nm).

Results. Detachment of the alkane sample from HOPG results in brittle fracture occurring close to the interface. After the detachment most of the HOPG surface is covered by a $C_{390}H_{782}$ layer of small nonuniform thickness. In areas where this film is several nanometers thick and flat, lamellar morphology similar to that of the surface of the detached sample can be seen. However, the resolution achievable by studying the surface of the detached alkane is better, and we therefore concentrate on the latter. Figure 1 displays selected areas showing typical features of the surface. The horizontal ribbons, ca. 41 nm in width, are in fact crystalline lamellae of extended alkane chains viewed edge-on.[16,17] Rhomboid-shaped protrusions and pits (missing blocks) are seen on the exposed lamellar sides. The height profiles underneath the images reveal that the steps are 0.5 nm in height, evidently corresponding to the thickness of one alkane chain. The appearance of the image is reminiscent of electron micrographs of fracture surfaces of extended-chain polyethylene crystals.[22] Similar morphology was observed by AFM in PE detached from HOPG surface.[18] On the thin PE layer which remained on the graphite, protrusions were found corresponding to the pits on the detached PE surface.[19,20]

The existence of protrusions in Figure 1 and in subsequent images implies that the majority of the area shown in these figures is not the first layer originally in contact with the graphite. This parallels the observation on PE.

From the inclination of the ridges bounding the protruding blocks and pits, one can conclude that the molecular chains are tilted with respect to the layer normal by ≈30°. This fits well with lamellar basal planes being {201}, assuming that the side faces, viewed flat on, are {110} planes. Furthermore, the measured average lamellar thickness of 41 nm fits well with the calculated value of 40.7 nm (parameters used are $L = 390 \times c/2 + 0.2 = 49.7$ nm, $a = 0.74$ nm, $b = 0.49$ nm, and $c = 0.254$ nm, where a, b, and c are unit cell parameters).

Figure 2a shows the morphology over a larger area in amplitude contrast. Three distinct orientations of the lamellae are visible, inclined at 60° to each other. As in PE crystallized on graphite[18−20] and in monolayers of alkanes,[12,17] the three orientations result from epitaxial relationship with the hexagonal lattice of graphite. As the chain tilt angle is close to 30°, there are no gaps between the domain boundaries.

In several places one can observe protrusions and pits which are shorter than the extended chain length L. In fact, most of those have a length close to $L/2$. They therefore most likely correspond to chains folded in two (F2). Selected areas **b** and **c** are shown enlarged in Figure 2b,c. In most cases the $L/2$ blocks start at the

† Polish Academy of Science.
‡ University of Sheffield.
* Corresponding authors: e-mail atracz@cbmm.lodz.pl, g.ungar@sheffield.ac.uk.

10.1021/ma050494q CCC: $30.25
Published on Web 05/14/2005

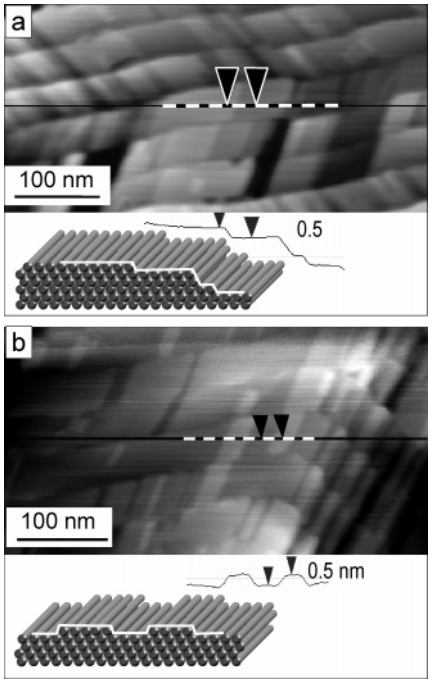

Figure 1. AFM height images of two selected areas of the fracture surface of alkane $C_{390}H_{782}$ crystallized from melt on graphite surface. Lamellae of tilted extended chains are seen edge-on. The height profiles at the bottom were scanned along the lines indicated.

bottom or the top edge of the lamellar side face (marked F2 and F2′ in Figure 2b,c). However, in certain places, such as that marked F2* and that between the two pits marked F4, the F2 blocks are in the middle. In those cases, the missing blocks appear to have consisted of chains folded in four (F4).

The protrusion marked F2″ is rather atypical and shows what appear to be F2 chains in a row inclined at ca. 30° to the underlying lamella. While most of the sample is relatively flat and covers a depth range of several nanometers only, there are areas where thicker chunks had detached, exposing deeper layers of the bulk alkane. Figure 3 shows such an area. There are three depth regions in Figure 3. The area marked as 1 had cleaved closest to the graphite substrate, and the area 2 is ca. 12 nm deep, while the region marked 3, appearing dark in Figure 3a, is more than 40 nm deep relative to region 1, as shown by the depth profile. The phase image in Figure 3b is that of the somewhat enlarged area framed in Figure 3a. While extended-chain lamellae are seen in area 1, once-folded chain (F2) lamellae are observed in area 3. Rather intriguingly, in area 2 thin lines are evident, running along the middle of the side faces, i.e., halfway between the two edges of what would be regarded in area 1 as extended chain lamellae.

Discussion. The results clearly demonstrate the versatility of the substrate detachment technique in AFM studies of polymer morphology at interfaces. They also illustrate the capability of the method of depth profiling on a very fine depth scale. Owing to the flatness of the exposed surface, the morphology of melt-crystallized long alkanes can now be studied in unprecedented detail.

Going on the experience of previous studies using bulk methods, observation of extended-chain crystals of $C_{390}H_{782}$ would not have been expected for a cooling rate of 10 °C/min. For example, a cooling rate 20 times lower

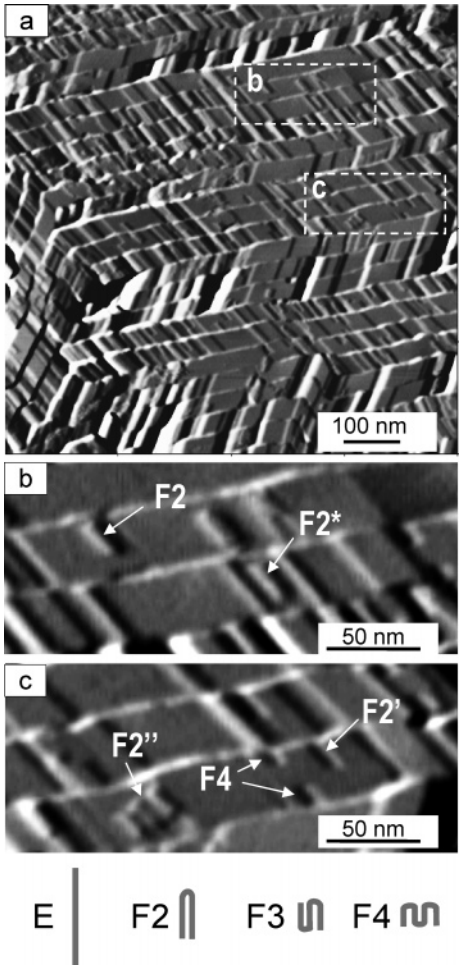

Figure 2. (a) Amplitude contrast image of a typical area of the fracture surface. (b) and (c) show enlarged areas marked **b** and **c** in (a). For description of labels see text.

did not produce amounts of extended chains detectable by either Raman LAM, DSC, or SAXS in bulk crystallization of $C_{390}H_{782}$.[14] It would appear therefore that the presence of the ordered extended-chain monolayer on the graphite surface above the bulk melting point had a nucleating effect at low supercoolings. Thus, even the slow-moving extended-chain growth front would have traveled a distance of a few nanometers from the nucleating layer by the time the F2 melting point was reached during the 10 °C/min cooling. The present observation is in line with the previous finding of similar 10 °C/min cooling experiments on PE, where it was found that near the graphite surface lamellar thickness was around 100 nm, a value unattainable in bulk crystallization under remotely similar conditions.

The presence of occasional F2 blocks on extended-chain lamellar edges in layers originally close to graphite has not been expected. Neither SAXS nor Raman LAM spectroscopy indicated their presence in previous bulk experiments. However, in view of their scarcity, their previous oversight is understandable.

The F2 blocks are narrow; in fact, it should be noted that, in the case of protrusions, their width is somewhat overestimated. This is due to the fact that the tip radius was ca. 10 nm. Conversely, the width of the pits is underestimated, and very narrow pits would have been unobserved. We propose that some folded chains could have been trapped during extended-chain crystallization, particularly if the fold or the chain ends were

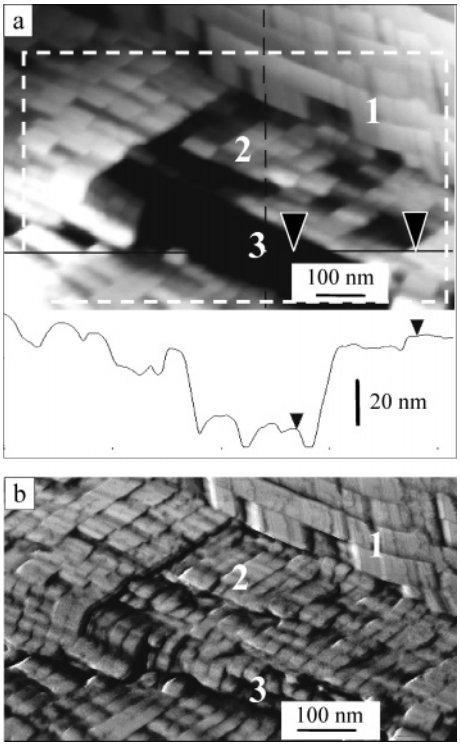

Figure 3. (a) Height image of an area of the fracture surface of $C_{390}H_{782}$ with regions of different depths. (b) Enlarged phase image of the framed area in (a). The surface in region 1 was closest to the graphite, that of region 2 was ca. 12 nm further away, and region 3 was >40 nm away from the graphite substrate (see profile). Extended-chain and once-folded (F2) lamellae are seen in regions 1 and 3, respectively. The lamellae in region 2 show a thin line halfway between the lamellar edges.

located at the bottom or the top edge of the lamellar side face, as indeed observed in the majority of cases in Figure 2. If surrounded by extended chains and complemented by a second F2 chain completing the lamellar traverse, such a deposition would have extra stability and could remain incorporated in the crystal. It is rather more difficult to account for the apparent presence of F4 chains.

We now turn to the features further away from the graphite surface, as revealed in Figure 3. In area 3 of that figure there is clear evidence that extended-chain crystallization had been replaced by folded-chain crystallization, as lamellar thickness is half that in area 1. Area 3 had therefore crystallized when the temperature fell below the F2 melting point T_m^{F2}. There is extensive evidence from previous work on alkanes ≤258 carbons long[2,3,15] that below T_m^{F2} the NIF form appears first. NIF consists of a mixture of once-folded (F2) and nonfolded half-crystalline chains, which traverse the crystalline lamella only once and whose cilia form an amorphous interlayer. Depending on the crystallization temperature T_c, NIF was found to transform subsequently to extended-chain (higher T_c) or F2 crystals (lower T_c). It may thus not be inappropriate to suggest that the "bilayer" lamellae in area 2 of Figure 3, apparently consisting of a mixture of extended and folded chains, had formed via the formation and subsequent thickening of NIF lamellae. According to this interpretation, a sizable proportion of F2 chains would have been trapped within the extended-chain lamellae in the thickening process (see Figure 4a). In the deeper layers (area 3), which formed at a lower T_c, NIF would

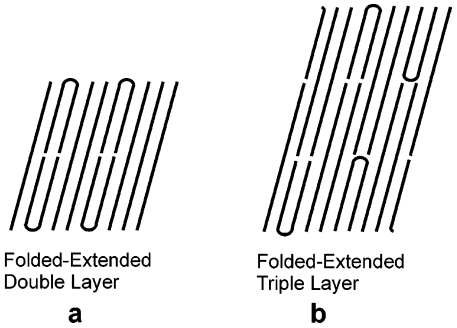

Figure 4. Schematic models of a stacking repeat unit (a) in the extended-chain lamellae with mixed-in folded chains (the double-layer folded−extended form) proposed here for the lamellae in region 2 of Figure 3b and (b) in bulk melt-crystallized alkanes with ca. 200 carbons (the triple-layer folded−extended form).[3]

have transformed to F2 lamellae, consistent with the earlier observations on alkanes such as $C_{246}H_{494}$.[15] The presence of F2 chains within E lamellae formed by NIF → E transformation would have easily been overlooked in SAXS experiments, since the enhanced even order diffraction peaks would have been mistaken for the presence of a proportion of separate F2 crystals. It should be noted that the extended-chain lamellae with mixed-in folded chains (the double-layer form, Figure 4a) proposed here is different from the triple-layer mixed folded−extended form established by X-ray, Raman,[3a] and neutron scattering[3b] in alkanes with ca. 200 carbons (Figure 4b).

This work has shown that a range of morphologies, formed during nonisothermal crystallization, can be observed at different distances from the substrate. Among other things, unexpected morphological features, such as trapped folded chains in otherwise extended-chain lamellae, have been identified. Furthermore, chain tilt is observed directly. It is clear that the substrate detachment technique has considerable potential in studies of polymer morphology. The morphological details revealed by the present preliminary study raise a number of intriguing questions which we are now investigating in detail.

Acknowledgment. We are very grateful to Dr. G. M. Brooke for the alkane samples and to financial support from Engineering and Physical Research Council and European Cooperation in the Field of Scientific and Technical Research (COST-P12).

References and Notes

(1) Ungar, G.; Zeng, K. B. *Chem. Rev.* **2001**, *101*, 4157−4188.
(2) Ungar, G.; Zeng, X. B.; Brooke, G. M.; Mohammed, S. *Macromolecules* **1998**, *31*, 1875−1879.
(3) (a) Ungar, G.; Zeng, X. B.; Spells, S. J. *Polymer* **2000**, *41*, 8775−8780. (b) Zeng, X. B.; Ungar, G. In *Highlights of ISIS Science*; Rutherford-Appleton Laboratory, 2004, submitted to *Macromolecules*.
(4) Rastogi, A.; Hobbs, J. K.; Rastogi, S. *Macromolecules* **2002**, *35*, 5861−5868.
(5) Ungar, G.; Organ, S. J. *Polym. Commun.* **1987**, *28*, 232−235.
(6) Gorce, J. P.; Spells, S. J. *Polymer* **2004**, *45*, 3297−3303.
(7) Klein, P. G.; Driver, M. A. N. *Macromolecules* **2002**, *35*, 6598−6612.
(8) Organ, S. J.; Keller, A. *J. Polym. Sci., Polym. Phys.* **1987**, *25*, 2409−2430.
(9) Hosier, I. L.; Bassett, D. C. *Polymer* **2000**, *41*, 8801−8812.
(10) Winkel, A. K.; Hobbs, J. K.; Miles, M. J. *Polymer* **2000**, *41*, 8791−8800.

(11) Sanz, N.; Hobbs, J. K.; Miles, M. J. *Langmuir* **2004**, *20*, 5989−5997.
(12) Magonov, S. N.; Yerina, N. A.; Ungar, G.; Reneker, D. H.; Ivanov, D. A. *Macromolecules* **2003**, *36*, 5637−5649.
(13) Putra, E. G. R.; Ungar, G. *Macromolecules* **2003**, *36*, 5214−5225.
(14) Ungar, G.; Stejny, J.; Keller, A.; Bidd, I.; Whiting, M. C. *Science* **1985**, *229*, 386−389.
(15) Ungar, G.; Keller, A. *Polymer* **1986**, *27*, 1835−1844.
(16) Gilbert, E.; Reynolds, P.; White, J. *J. Appl. Crystallogr.* **2000**, *33*, 744−748.
(17) Magonov, S. N.; Yerina, N. A. *Langmuir* **2003**, *19*, 500−504.
(18) Tracz, A.; Jeszka, J. K.; Kucinska, I.; Chapel, J. P.; Boiteux, G.; Kryszewski, M. *J. Appl. Polym. Sci.* **2002**, *86*, 1329−1336.
(19) Tracz, A.; Kucinska, I.; Jeszka, J. K. *Macromolecules* **2003**, *36*, 10130−10132.
(20) Takenaka, Y.; Miyaji, H.; Hoshino, A.; Tracz, A.; Jeszka, J. K.; Kucinska, I. *Macromolecules* **2004**, *37*, 9667−9669.
(21) Brooke, G. M.; Burnett, S.; Mohammed, S.; Proctor, D.; Whiting, M. C. *J. Chem. Soc., Perkin Trans. 1* **1996**, 1635−1645.
(22) Wunderlich B.; Melillo, L. *Makromol. Chem., Macromol. Chem. Phys.* **1968**, *118*, 250−264.

MA050494Q